JOURNAL OF CATALYSIS 32, 304–314 (1974)

The Kinetics and Mechanism of Spillover

R. B. LEVY AND M. BOUDART*

Stauffer Laboratories of Chemistry and Chemical Engineering,
Stanford University, Stanford, California 94305

Received May 31, 1973

The rate of reduction r of WO_3 to H_xWO_3 ($x \sim 0.35$) by H_2 at room temperature was studied in mechanical mixtures of WO_3 with supported or unsupported Pt catalysts and in the presence of co-catalysts with varying proton affinity (PA). As PA increased, r decreased in the order: H_2O, CH_3OH, C_2H_5OH, n-C_3H_7OH, n-C_4H_9OH, t-C_4H_9OH. For these co-catalysts, r did not change with Pt surface area S. It did not change as the amount n of adsorbed co-catalyst was decreased to about a monolayer below which r fell linearly with n. For a co-catalyst with low PA, such as CH_3COOH, r depended on S. For co-catalysts with high PA, log r was proportional to PA over three decades of r. It appears that a solvated proton is formed on the metal. If PA is low, this is the rate determining process (rdp). But if PA is high, the rdp is shifted to the end of the reduction following the last surface migration of the proton in the adsorbed monolayer of co-catalyst, as the proton is released to the WO_3 surface. This model explains why H_2 spillover can be a fast process at low temperatures.

INTRODUCTION

In a mixture between a metal that can dissociatively adsorb a diatomic molecule and a nonmetal which itself cannot dissociate the molecule at the temperature of observation, the metal can act as a source of atoms which migrate to the nonmetal and participate there in various processes: oxidation, reduction or adsorption. Such a transport of atoms from the dissociating to the nondissociating surface has been called spillover (*1*). It has received wide attention in the last decade (*1–12*), in systems ranging from the high temperature Pt catalyzed oxidation of graphite (*7*) to the low temperature Pt catalyzed reductions of CuO (*1*) and WO_3 (*4, 5*). However, the nature of the transported species and the energetics of spillover are not understood.

One of the difficulties encountered in an explanation of the transport is the large binding energy between the metal and the adatom. For a dissociative exothermic adsorption this energy is at least as large as one half of the bond dissociation energy of the molecule. The temperature at which transport can be observed will depend on how the metal–adatom bond is broken. Thus, if the bond must be broken to form a free hydrogen atom, to obtain one such event per site per minute requires temperatures greater than 800 K. This estimate is for a unimolecular rate process (*13*) with an activation energy of 52 kcal mol^{-1}, one half of the dissociation energy of H_2 (*14*). To observe transport at lower temperatures a new bond has to be formed in the same elementary process in which the metal–adatom bond is broken. Determination of the nature of this new bond should help to understand spillover at low temperature. The present study explored this problem for one of the most dramatic examples of low temperature spillover, the platinum catalyzed reduction of WO_3 to H_xWO_3 ($x \sim 0.35$) at room temperature.

The reduction of WO_3 with H_2 at room temperature was first noted by Khoobiar (*4*) who observed the appearance of a

---

* To whom correspondence should be addressed.

blue color when a mechanical mixture of $Pt/\gamma Al_2O_3$ and WO_3 powders was exposed to hydrogen gas. Temperatures above 500 K were required to observe reduction in the absence of Pt. Further work by Benson, Kohn and Boudart (*5*) revealed that besides platinum, water was also required as a co-catalyst to observe the reduction at room temperature. If no water was admitted to the system or formed on the Pt surface no reduction was observed. The essential role of water was later confirmed by Boudart, Vannice and Benson (*1*): when D was replaced by H either in the water or in the reducing gas the rate of the reduction was decreased. Boudart, Vannice and Benson also found that methanol could be replaced by water in the reduction of the $Pt–WO_3$ mixture. Finally, they observed that a tenfold change in the platinum content of the mixture did not affect the course of the reduction indicating that the rate determining process of the reduction is occurring away from the platinum surface. To pinpoint the rate determining process, Vannice, Boudart and Fripiat (*15*) studied by NMR the mobility of protons in H_xWO_3 but found that it was so high that it could not be the rate determining process of the WO_3 reduction.

The room temperature reduction of WO_3 is unusual in that water is not a product of the reaction. Hydrogen penetrates the WO_3 matrix to form the hydrogen analog of the tungsten bronzes. Thus, it is possible to study the role of water and other vapors in the spillover taking place in the reduction of WO_3 at low temperature. The latter was followed volumetrically and gravimetrically in the presence of a number of proton acceptors as co-catalysts. This has enabled us to understand the role of the co-catalysts in making spillover possible at room temperature.

EXPERIMENTAL METHODS

The apparatus (Fig. 1) consisted of three interconnected units: a volumetric adsorption unit to measure the amount of hydrogen admitted to the reaction system (*5*), a constant pressure unit to follow the hydrogen uptake, and a gravimetric unit to determine the amount of vapor adsorbed on the catalyst–oxide mixture. The constant pressure unit was similar to that used earlier (*16*) except that the photocell was located on the arm of a mercury manometer and not directly on the gas volumetric system, to control the pressure better and faster. In the gravimetric unit, a Cahn RG-HV-2002 electrobalance was connected to the rest of the system by flexible steel

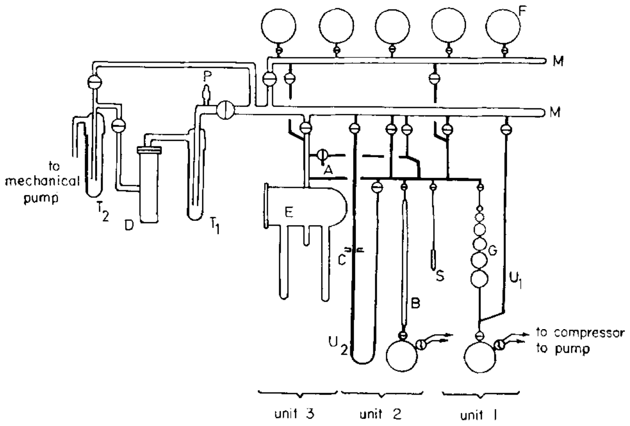

FIG. 1. Schematic diagram of the volumetric and gravimetric system used to study the WO_3 reduction. (A) Exit to transport agent storage bulbs; (B) graduated burette; (C) photocell controlling constant pressure system; (D) oil diffusion pump; (E) Cahn electrobalance; (F) gas storage bulbs; (G) calibrated gas bulbs; (M) manifolds; (P) Phillips pressure gage head; (S) sample holder; (T_1, T_2) liquid nitrogen traps; (U_1, U_2) manometers.

bellows to minimize the effect of vibrations. Fractions of a monolayer were easily detected in our large surface area samples (15 to 30 m^2 g^{-1}).

All three units had independent gas supply lines and could be equilibrated separately with the vapors of the transport agents used in the reduction. The manifold was pumped by a 100 liters s^{-1} oil diffusion pump backed by a 75 liters min^{-1} mechanical pump. Each pump was isolated from the manifold by liquid nitrogen traps. Due to the conductance of 5 liters min^{-1} of the trap between diffusion pump and manifold, the lowest pressure obtained at the entrance of the manifold was 10^{-7} Torr. The limiting conductance of the stopcocks and glass tubing increased this pressure to 10^{-3} Torr at the entrance to the sample holder S. This holder was separated from the other parts of the system by a powdered gold trap to avoid contamination by mercury vapor.

Materials

The tungsten trioxide was prepared from Matheson, Coleman and Bell reagent tungstic acid (*5*). Two catalysts were used for the reduction. Platinum black from Engelhard Industries, reported as 100% pure, was used as received. It had a surface area of 30 m^2 g^{-1} determined after a mixture of platinum and quartz powders had been heated to 100°C for 12 hr to simulate the reoxidation pretreatment of the WO_3–platinum mixtures. Platinum supported on SiO_2 prepared according to the method of Benesi, Curtis and Studer (*17*) contained 2.5% Pt with a dispersion (ratio of surface to total Pt atoms) of 0.58 (*18*). A mixture of supported catalyst and WO_3 powder in a 7:93 weight ratio had a total BET surface area of 30 m^2 g^{-1}. Such a mixture will be described in the text as 7% (Pt/SiO_2) + WO_3. Hydrogen was Ultra High Purity from Matheson Co., reported as 99.999% pure and containing less than 1 ppm oxygen. It was passed through a 3A zeolite trap cooled to liquid N_2 temperature before use. Further purification was not necessary because neither O_2 nor N_2 were poisons in our system. Oxygen used in the reoxidation was Matheson Co. Research Grade. Helium Grade A gas was used for dead volume determination. The oxygen and helium were passed over 3A zeolite at room temperature before use.

All alcohols were Reagent Grade Matheson Coleman and Bell chemicals. The acetic acid was Glacial Reagent from Baker and Adamson. All organic liquids were dried over 3A zeolite for several days and subjected to 4 to 5 cycles of the following degassing sequence: freezing to liquid N_2 temperature, pumping, thawing to room temperature with expansion of the vapors into the large manifold volume, pumping of the vapors and refreezing. In addition to the zeolite drying, *t*-butanol was dried over $LiAlH_4$ for several days, and acetic acid was mixed with a few drops of acetic anhydride to remove any traces of water present.

Procedure

The desired amount of catalyst and tungsten trioxide powders was ground for 30 min in a mortar. One mixture was used for a sequence of runs. Reproducibility of these runs was checked periodically by using the reduction in the presence of water as a standard. The procedure used in each run was the following: (1) The evacuated mixture was exposed to the vapors of the co-catalyst at room temperature. The equilibrium pressure was measured in manometer U_1 (Fig. 1) and read with a cathetometer. Equilibrium was reached when pressure and the weight recorded by the microbalance reached stable values. It was achieved in less than 30 min regardless of vapor pressure. Temperature fluctuations did not exceed 0.4 K in the course of a run. Only the results of the reduction in the presence of methanol and *t*-butanol were affected by such fluctuations because of the high vapor pressure of these transport agents. For methanol this made reproducible measurement of the reduction rate impossible. (2) Hydrogen was introduced into unit 2 after determination of the initial number of moles admitted to the system. This was followed by a change in volume of burette B until the desired total pressure was achieved. During this period unit 2 was isolated from the sample holder S. The total pressure used in most runs was 300 Torr. (3) The H_2 and co-catalyst vapor were exposed to the Pt–WO_3 mixture which had already been equilibrated with the vapor in step 1. The reduction was performed at 294 K and followed for 60–120 min. In a few cases the reduction was followed for several hours to determine the maximum uptake of hydrogen. (4) Once the reduction was complete the sample was evacuated and exposed to 400 Torr oxygen at room temperature. Within 4 hr the sample was reoxidized and returned to the characteristic color of the original mixture. The exposure to oxygen was done slowly to avoid excessive local heating. (5) The mixture was dried by evacuation at 373 K for 4 hr. Infrared spectra show that such a treatment is adequate to remove water adsorbed on the surface after the reoxidation (*15*).

The structure of both reduced and reoxidized samples was checked by X-ray diffraction. The diffraction peaks and intensities of the lines in the pattern of the reoxidized sample agreed well with reported values for WO_3 (*19*). The blue reduced sample exhibited a diffraction pattern typical of H_xWO_3 with x between 0.3 and 0.4 (*19*).

RESULTS

The influence of the chemical nature of the co-catalyst on the reduction of WO_3 is shown on Fig. 2. The curves represent the hydrogen uptake as a function of time for a 2.5% Pt + WO_3 mixture after exposure to different co-catalysts at 294 K. The effect of Pt surface area on the rate of reduction was determined by following the reduction of four different mixtures in the presence of acetic acid, water, *n*-propanol, *n*-butanol, and *t*-butanol. The mixtures were: 10% Pt + WO_3, 2.5% Pt + WO_3, 7% (Pt/SiO_2) + WO_3 and 1.8% (Pt/SiO_2) + WO_3, with Pt surface areas of 3, 0.75, 0.24 and 0.06 m^2 g-mixture^{-1}, respectively. After some sintering the samples containing Pt Black gave reproducible results for the subsequent reductions. Reproducibility was achieved for all runs with the 7% (Pt/SiO_2) + WO_3 sample (0.24 m^2 Pt g^{-1}). On the other hand, the sample with 0.06 m^2 Pt g^{-1} showed a large decrease of the rate of reduction in the presence of water after treatment with any of the alcohols. Due to this apparent poisoning no further tests were performed with this sample. Typical hydrogen uptake vs time curves are shown in Figs. 3 and 4. To compare the H_2 uptake of samples with such different Pt surface areas, the data were corrected for the uptake of H_2 by the Pt surface. In such a correction care had to be taken to account for the sintering of the platinum powder during the first reoxidation of the sample. The amount of H_2 adsorbed on Pt in the initial run was calculated using the stoichiometry of Benson and Boudart (*20*) and the initial Pt surface area. The sintering was determined from the constant difference in the uptake vs time curves between the first and subsequent reductions. It amounted to a 40% decrease in Pt surface area. The correction applied to the results, expressed relative to the H_2 uptake of the 7% (Pt/SiO_2) sample, was 10 and 60 μmol g^{-1} of WO_3 for

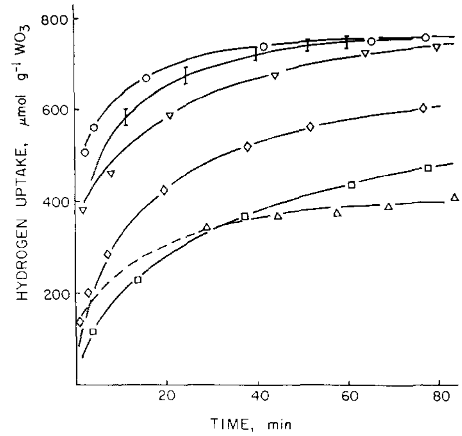

FIG. 2. Hydrogen uptake by a 2.5% Pt + WO_3 mixture at 295 K in the presence of various co-catalysts: (○) H_2O, (I) MeOH, (▽) EtOH, (◇) *n*-PrOH, (□) *n*-BuOH, (△) *t*-BuOH. All runs performed at high values of adsorption of co-catalyst (saturated vapor) and constant hydrogen pressure (300 Torr).

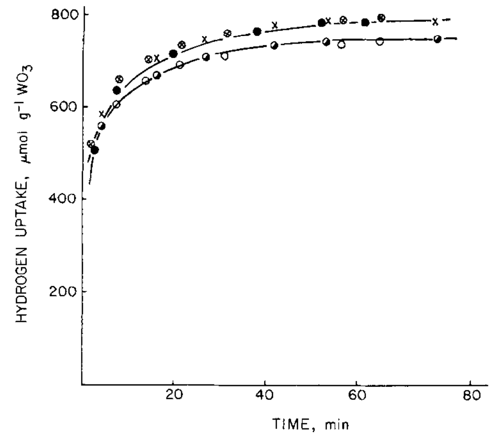

FIG. 3. Hydrogen uptake by WO_3 in the presence of water (saturated vapor) and different amounts of platinum: (●) 7% (Pt/SiO_2), (◑) 2.5% Pt, (○) 10% Pt. For the Pt samples the uptake is corrected for hydrogen sorbed on Pt: 10 μmol g^{-1} of WO_3 for 2.5% Pt and 60 μmol g^{-1} of WO_3 for 10% Pt. The crosses show that by increasing the 2.5–10% Pt curve by a factor of 1.07 all three curves become identical.

the 2.5 and 10% Pt + WO_3 mixtures, respectively.

A tenfold change in the Pt surface area did not affect the rate of reduction with water as a co-catalyst (Fig. 3). In the presence of water all reductions proceeded with a fast initial hydrogen uptake followed by a slower uptake that reached saturation at approximately 0.35 H per WO_3. However, the final H_2 uptake of the reduction catalyzed by Pt/SiO_2 was larger than the final uptake of the reductions catalyzed by Pt black. The difference of 7% was small compared to the large differences in surface areas. If the hydrogen uptakes of the 2.5 and 10% samples are increased by 7% for the entire course of the reduction, the three curves become identical, as shown by the crosses in Fig. 3. This result suggests that not all of the WO_3 in the Pt black mixtures is available for reduction in the time scale of our experiments. In this connection, let us mention two observations made in this laboratory (*21*). In one experiment a disk of WO_3 containing a small piece of Pt wire at its center was exposed to wet H_2. The blue color characteristic of H_xWO_3 slowly developed concentrically around the Pt. It was evident that hydrogen diffusion between WO_3 particles was very slow. In another experiment, when WO_3 was separated from the platinum altogether by placing the two powders at opposite ends of a U-shaped glass tube, no reduction took place even after 2 yr.

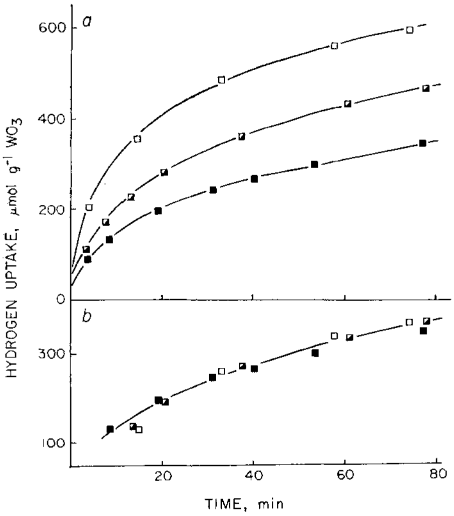

FIG. 4a. Hydrogen uptake by WO_3 in the presence of *n*-BuOH (saturated vapor) and different amounts of platinum: (■) 7% (Pt/SiO_2), (◩) 2.5% Pt, and (□) 10% Pt. (b) Same points as (a) after cancelling the initial hydrogen uptake: (◩–■) = 90 μmol g^{-1} of WO_3, (□–■) = 240 μmol g^{-1} of WO_3.

Figure 4a shows the reduction in the presence of *n*-BuOH. In contrast to Fig. 3, where the influence of Pt surface area on the rate of the initial hydrogen uptake region ($t < 2$ min) could not be resolved, the slower reduction with *n*-BuOH shows that an increase in the Pt surface area increases the rate of initial hydrogen uptake. However, when this increase is subtracted from the balance of the reduction by sliding the vertical scales (Fig. 4b), all the reduction curves coincide. This shows that the Pt surface area effect present at the beginning of the reduction changes as the reduction proceeds. A tenfold increase in Pt surface area again leaves the rate of the slow region of the reduction unaffected. A similar behavior was found for *n*-PrOH and *t*-BuOH. Acetic acid, on the other hand, did not follow this pattern. The re-

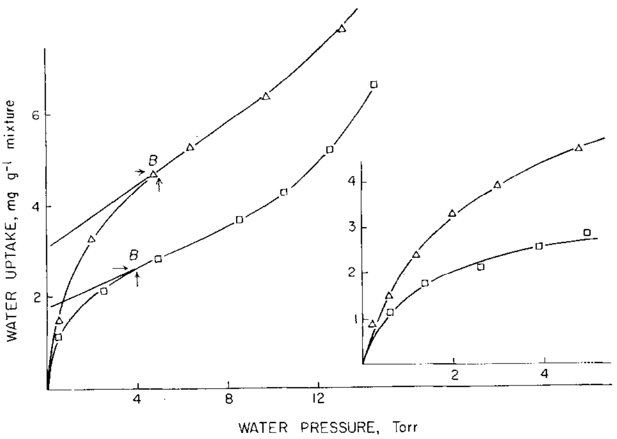

FIG. 5. Adsorption of water at 294 K on 7% (Pt/SiO_2) + WO_3 (△) and 2.5% Pt + WO_3 (□).

duction catalyzed by 2.5% Pt was similar to that in the presence of *n*-PrOH. However, when the Pt surface area was increased by a factor of four the two co-catalysts behaved very differently. In the presence of acetic acid, as the surface area of platinum was increased, the reduction was faster in the initial as well as the final regions, suggesting that the effect of surface area persisted during the entire course of the reduction.

All the runs reported in Figs. 2–4 were performed after exposure to the saturated vapor pressure of the co-catalysts. The effect of amount of co-catalyst adsorbed on the rate of reduction was determined by varying the pressure of the co-catalyst to which the mixture was exposed before reduction. The amount adsorbed corresponding to this pressure was obtained from the adsorption isotherms of the co-catalyst. Figure 5 shows adsorption isotherms of water on two samples, 2.5% Pt + WO_3 and 7% (Pt/SiO_2) + WO_3. Figures 6 and 7 show the H_2 uptake vs time curves for the reduction of these two samples at various H_2O pressures. Figures 6 and 7 indicate that only below a water pressure of 4 Torr does water coverage have an effect on the rate of reduction of WO_3.

The effect of the hydrogen pressure on the reduction rate was determined by running the reduction in the presence of water at 300 and 600 Torr total pressure. The H_2 uptake vs time curves were identical.

To determine the effect of the temperature on the hydrogen uptake after apparent saturation, a hydrogen tungsten bronze sample formed in one of the above reductions was heated after evacuation. No hydrogen evolution was observed until a temperature of 373 K was reached. At this temperature the bronze started to decompose. At 523 K, the decomposition was complete.

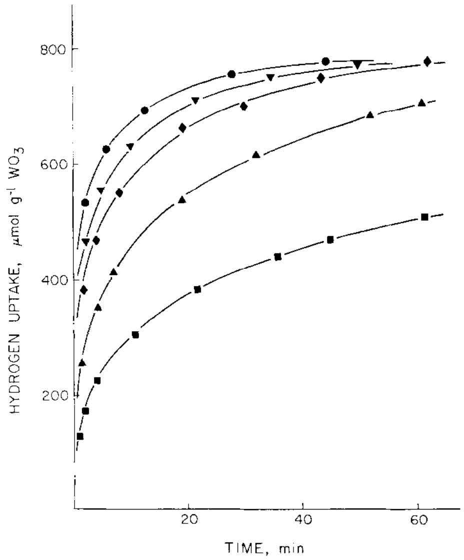

FIG. 6. Hydrogen uptake by a 2.5% Pt + WO_3 mixture after exposure to various pressures of water vapor: (●) 4, 8 and 18 Torr; (▼) 1.6 Torr; (♦) 0.8 Torr; (▲) 0.4 Torr; (■) 0.25 Torr.

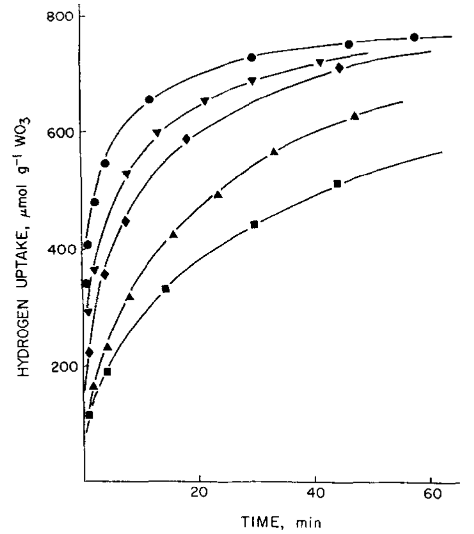

FIG. 7. Hydrogen uptake at 295 K by a 7% (Pt/SiO_2) + WO_3 mixture after exposure to various pressures of water vapor: (●) 4 and 18 Torr; (▼) 3 Torr; (◆) 1.8 Torr; (▲) 1.1 Torr; (■) 0.6 Torr.

DISCUSSION

The results of Fig. 2 show that many substances can be used as co-catalysts for hydrogen spillover in the reduction of WO_3 but the uptake of H_2 at a given time is influenced by the nature of the co-catalyst. To obtain kinetic information from these data, we note that the experimental uptake curves show two regions corresponding to an initial fast H_2 uptake followed by a slower uptake leading to saturation. As quantitative data can be obtained only from the slower region, we will concentrate on this region in the following analysis.

The degree of advancement of the reduction is defined by

$$\alpha = \frac{H_2 \text{ uptake at } t}{H_2 \text{ uptake at } t = \infty}. \qquad (1)$$

Our data in the slow region are described very well by a damped Elovich equation:

$$\frac{d\alpha}{dt} = k_0[\exp(-K\alpha e^{-\gamma/\alpha})](1 - \alpha). \qquad (2)$$

With the same value of the constant K for all the experiments ($K = 10$), only small variation in the damping constant γ is necessary to obtain good fit of the data. A typical result is shown in Fig. 8, where the integral of the concentration dependent part of Eq. (2) is plotted as a function of time. The lower limit of the integration is arbitrary. Changing this limit shifts the intercept of the line without changing its slope. The slope of the line is the rate constant k_0. It represents the rate of reduction that would be observed at zero concentration if the mechanism that controls the slow reduction were obeyed throughout the reaction. Such an extrapolation is shown in Fig. 9. A possible theoretical significance of the damped Elovich equation may be found elsewhere (*22*). For our present purposes, this equation will simply be used as a convenient way to characterize the reduction by means of k_0 because at zero concentration we avoid ill-understood effects of bulk hydrogen–hydrogen interactions on the rate of formation of the H_xWO_3 phase.

Table 1 summarizes the results of the kinetic analysis. The rate constant k_0 is seen to be independent of a fourfold change in Pt surface area for water and the alcohols used in this study. Furthermore, the rate constants decrease for increasing size and branching of the alkyl group of the alcohols. Such a systematic change in properties is precisely what is observed for the proton affinity of these molecules (*23*, *24*).

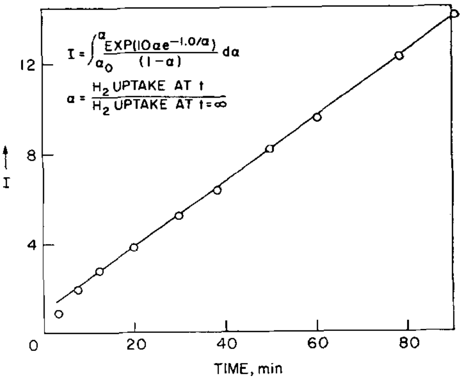

FIG. 8. Reduction of a 2.5% Pt + WO_3 mixture at 295 K in the presence of saturated *n*-butanol vapor. Data plotted according to Eq. (2) with $I = \int_{0.066}^{\alpha} \{[\exp(10\alpha e^{-1.0/\alpha})]/(1 - \alpha)\} d\alpha$.

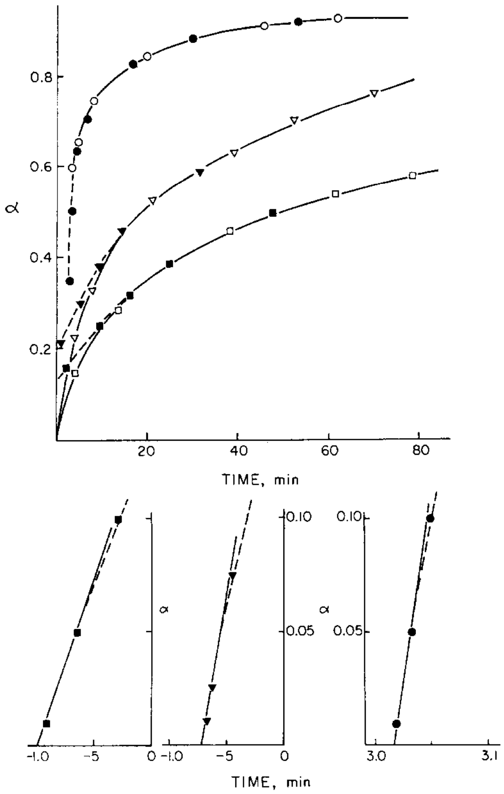

FIG. 9a. Comparison between experimental hydrogen uptake (open points) and values calculated with Eq. (8) (closed points). Reduction of a 2.5% Pt + WO_3 mixture in the presence of H_2O (●), *n*-PrOH (◆), and *n*-BuOH (■). (b) Extrapolation to $\alpha = 0$ showing the initial rate, k_0.

TABLE 1

RATE CONSTANTS FOR THE WO_3 REDUCTION

Co-catalyst	Catalyst % Pt black	Factor γ in Eq. (2)	Rate constant ($\times 10^3\ s^{-1}$)
Water	2.5	0.5	58.2
	10	0.5	58.2
Ethanol	2.5	1.5	1.5
n-Propanol	2.5	1.5	0.50
	10	1.5	0.66
n-Butanol	2.5	1.0	0.25
	10	1.5	0.33
t-Butanol	2.5	1.0	0.075

TABLE 2

THERMOCHEMICAL DATA FOR THE CO-CATALYSTS

Co-catalyst: S	$HA(S^+)$[a] (kcal mol^{-1})	IP(S)[b] (eV)	Proton affinity PA(S) (kcal mol^{-1})	Rate constant $k° \times 10^3\ s^{-1}$ 2.5% Pt + WO_3
H_2O			164[c]	58.2
MeOH	117	10.85	180[d]	
EtOH	114	10.48	186[d]	1.5
n-PrOH	(116)	10.20	193[e]	0.5
n-BuOH	(116)	10.04	197[e]	0.25
t-BuOH	(116)	9.70	206[e]	0.075

[a] $HA(S^+)$ = hydrogen affinity of S^+, data from J. L. Beauchamp and M. C. Caseiro, *J. Amer. Chem. Soc.* **94**, 2638 (1972).

[b] IP(S) = ionization potential of S, data from J. L. Franklin, J. D. Dillard, H. M. Rosenstock, J. T. Herron, K. Daxal and F. H. Field, "*Ionization Potentials, Appearance Potentials and Heats of Formation of Gaseous Positive Ions*," NSRDS-NBS, 26, U. S. Govt. Printing Office, Washington, DC, 1969.

[c] J. L. Beauchamp, *Annu. Rev. Phys. Chem.* **22**, 527 (1971).

[d] J. L. Beauchamp and M. C. Caseiro, *J. Amer. Chem. Soc.* **94**, 2638 (1972).

[e] Calculated from a thermochemical cycle expressed by the relation $PA(S) = HA(S^+) + IP(H) - IP(S)$ where IP(H) is the ionization potential of H [13.6 eV, from Ref. (b)].

The value of these affinities as well as the thermochemical data used in calculations are shown in Table 2. The rate constants for the reduction of the 2.5% Pt + WO_3 mixture are also shown for comparison. The correlation between rate of reduction and proton affinity of the co-catalyst suggests the formation of a solvated proton on the metal followed by proton transport in the adsorbed phase of the co-catalyst to the reduction site on the oxide.

After a fast H_2 chemisorption on Pt which, at the pressures and temperatures used in this work, leads to saturation of the surface with atoms (*25*), the co-catalyst reacts with the hydrogen to form a solvated proton. The electron is left behind in the metal. The large proton affinity of the co-catalyst provides the energy necessary to create the proton. An estimate of the energies involved in the formation of a solvated proton from a chemisorbed hydrogen atom and water shows that, in fact, this process is exothermic (*22*). Details of this calculation will be included in a subsequent publication. The observation that for water and the alcohols the rate of reduction of WO_3 is independent of Pt surface area shows that the formation of the solvated proton on the Pt surface is not rate determining for these co-catalysts. Formation of the solvated proton is followed by fast proton diffusion in the adsorbed layer to the reduction site, with a coefficient characteristic of proton diffusion through a water or alcohol layer (*26*). At the reduction site the co-catalyst releases the proton which then crosses the WO_3 surface and diffuses into the solid. Since this last process was shown to be fast (*15*), we conclude, by elimination, that the release of the proton with interfacial crossing is rate determining. The rate constant k_0 then contains an activation energy which will be proportional to the proton affinity. Thus, a plot of ln k_0 vs proton affinity should give a straight line. This is indeed the case, as shown in Fig. 10. The relatively small slope of 0.16 reflects the attenuation of the influence of chain length on the proton affinity possibly as a result of the interaction of the co-catalysts with the solid surface. The quantitative correlation of Fig. 10 is offered as a strong argument in support of our model of spillover. But there are other arguments.

Thus, as the proton affinity of the co-catalyst is reduced, the solvation energy decreases until the formation of the complex at the Pt surface becomes rate determining. Then the rate will become dependent on Pt surface area, which was observed for the reductions in the presence of acetic acid.

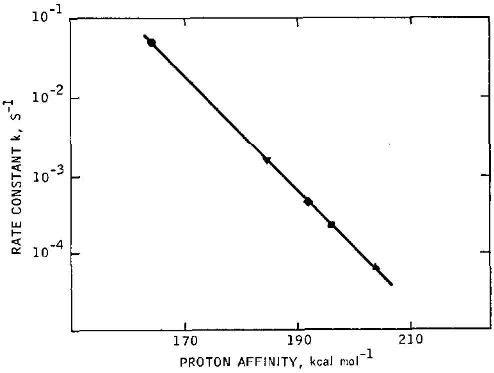

FIG. 10. Dependence of the rate constant k_0 on the proton affinity of the transport agent for H_2O (●), EtOH (▼), *n*-PrOH (◆), *n*-BuOH (■), and *t*-BuOH (▲).

Another argument rests on the observed changes of rate at low coverage of the surface by the co-catalyst. So far, we have discussed cases of high coverage of the surface by the co-catalyst. As the amount of co-catalyst on the surface is reduced, diffusion in an incomplete monolayer of the solvated proton from Pt to the reduction site on the WO_3 surface may become rate determining. Figures 6 and 7 show that only below a minimum pressure does the coverage have an effect on the rate. This minimum pressure corresponds to the point (marked B in Fig. 5) used to estimate monolayer coverage (*27*). Consequently, it appears that the rate is surface diffusion limited only when the amount of co-catalyst becomes insufficient to form a monolayer. In this diffusion controlled regime we expect the dimensionless flux, expressed as total hydrogen uptake F divided by source concentration C_0 and source perimeter A_0, to be proportional to dimensionless time (*8*). Therefore, at constant time we expect the uptake to be proportional to source concentration. In our system this source concentration can be determined from the equilibrium relationship of the proton solvation:

$$\text{Pt–H} + n\text{S} \rightleftarrows \text{Pt}^- + \text{S}n\text{H}^+, \qquad (3)$$

where S represents the co-catalyst, and n the number of co-catalyst molecules associated with each proton.

The uptake F will therefore be proportional to the nth power of the co-catalyst concentration. Figure 11 shows a doubly logarithmic plot of hydrogen uptake vs co-catalyst coverage for the reduction in the presence of water. Below monolayer coverage a straight line with slope n equal to unity is obtained. This value confirms our initial implicit assumption that only one co-catalyst molecule is associated with each proton. Therefore gas phase proton

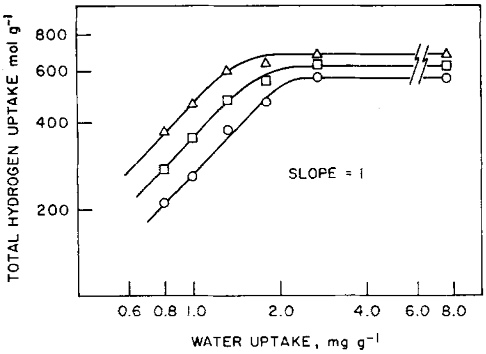

FIG. 11. Reduction of a 2.5% Pt + WO_3 mixture in the presence of water. Diffusion analysis at constant uptake times with varying water coverage. Diffusion controlled reduction at low transport agent coverage. Uptake at times: (○) 5 min; (□) 10 min; (△) 20 min; sample, 2.5% Pt black–WO_3.

affinities of Table 2 are applicable, as is indeed shown empirically by Fig. 10.

In summary, our model for hydrogen spillover explains all observations on the rate of reduction of WO_3, in particular the increase in rate with increasing proton affinity of the co-catalyst, the lack of dependence of the rate on platinum surface area for co-catalysts of high proton affinity, the lack of dependence of the rate on hydrogen pressure when the platinum surface is saturated with hydrogen, and the dependence of the rate on amount of adsorbed co-catalyst below monolayer coverage.

According to the model the energy required to break the bond between the metal and the chemisorbed hydrogen atom is compensated by the formation of a solvated proton after the chemisorbed hydrogen loses its electron to the conduction band of the metal. The co-catalyst acts as proton acceptor and the transported species is the solvated proton. This solvated proton diffuses from the metal surface to the surface of WO_3 where the proton is released to the reduction site.

ACKNOWLEDGMENTS

This work was supported by the National Science Foundation under Grant GK 17451X and by the Center for Materials Research at Stanford University. We thank J. E. Benson for many stimulating discussions and his permission to use some of his unpublished data referred to in this paper. The assistance of John Brauman in guiding us through the data on proton affinity is also gratefully acknowledged.

REFERENCES

1. BOUDART, M., VANNICE, M. A., AND BENSON, J. E., *Z. Phys. Chem. N.F.* **64**, 171 (1969).
2. SINFELT, J. H., AND LUCCHESI, P. T., *J. Amer. Chem. Soc.* **85**, 3365 (1963).
3. LUCCHESI, P. T., CARTER, J. L., AND SINFELT, J. H., *J. Amer. Chem. Soc.* **86**, 1494 (1964).
4. KHOOBIAR, S., *J. Phys. Chem.* **68**, 411 (1964).
5. BENSON, J. E., KOHN, H. W., AND BOUDART, M., *J. Catal.* **5**, 307 (1966).
6. CARTER, J. L., LUCCHESI, P. J., CORNEIL, D. J. C., AND SINFELT, J. H., *J. Phys. Chem.* **69**, 3070 (1965).
7. L'HOMME, G. A., BOUDART, M., AND D'OR, L., *Bull. Acad. Roy. Belg. Cl. Sci.* **52**, 1206 (1966).
8. ROBELL, A. J., BALLOU, E. V., AND BOUDART, M., *J. Phys Chem.* **68**, 2748 (1964).
9. SERMON, P., AND BOND, G. C., *Catal. Rev.* **8**, 211 (1973).
10. VANNICE, M. A., AND NEIKAM, W. C., *J. Catal.* **20**, 260 (1971); *Int. Congr. Catal., 5th,* Prepr. No. 41, 1972.
11. SCHLATTER, J. C., AND BOUDART, M., *J. Catal.* **24**, 482 (1972).
12. ROMAN, A., AND DELMON, B., *C. R. Acad. Sci.* **273**, 94 (1971).
13. BOUDART, M., "Kinetics of Chemical Processes." Prentice-Hall, Englewood Cliffs, NJ, 1968.
14. EGGERS, D. F., JR., GREGORY, N. W., HALSEY, G. D., JR., AND RABINOVITCH, B. S., "Physical Chemistry." Wiley, New York, 1964.
15. VANNICE, M. A., BOUDART, M., AND FRIPIAT, J. J., *J. Catal.* **17**, 359 (1970).
16. BOUDART, M., ALDAG, A. W., AND VANNICE, M. A., *J. Catal.* **18**, 46 (1970).
17. BENESI, H. A., CURTIS, R. M., AND STUDER, H. P., *J. Catal.* **10**, 328 (1968).
18. MADON, R. J., unpublished data.
19. "Powder Diffraction File," Joint Committee on Powder Diffraction Standards, Amer. Soc. for Testing and Materials, 1969.
20. BENSON, J. E., AND BOUDART, M., *J. Catal.* **4**, 704 (1965).
21. BENSON, J. E., unpublished data.
22. LEVY, R. B., PhD dissertation, Stanford, 1972.
23. BEAUCHAMP, J. L., AND CASEIRO, M. C., *J. Amer. Chem. Soc.* **94**, 2638 (1972).

24. Brauman, J. I., Riveros, J. I., and Blair, L. K., *J. Amer. Chem. Soc.* **93**, 3924 (1971).
25. Vannice, M. A., Benson, J. E., and Boudart, M., *J. Catal.* **16**, 348 (1970).
26. Touillaux, R., Salvador, P., Vanmeersche, C., and Fripiat, J. J., *Isr. J. Chem.* **6**, 337 (1968).
27. Sing, S. J., and Gregg, K. S. W., "Adsorption, Surface Area and Porosity." Academic Press, New York, 1967.